THE JOURNAL OF BIOLOGICAL CHEMISTRY
Vol. 280, No. 25, Issue of June 24, pp. 23464–23474, 2005
Printed in U.S.A.


# Different Structural Requirements for the Constitutive and the Agonist-induced Activities of the $\beta_2$-Adrenergic Receptor*

Received for publication, March 16, 2005
Published, JBC Papers in Press, April 21, 2005, DOI 10.1074/jbc.M502901200

**Caterina Ambrosio‡, Paola Molinari‡, Francesca Fanelli§, Yoshiro Chuman¶‖, Maria Sbraccia‡, Ozlem Ugur**, and Tommaso Costa‡ ‡‡**

*From the ‡Department of Pharmacology, Istituto Superiore di Sanità, Viale Regina Elena 299, Rome 00161, Italy, the §Dulbecco Telethon Institute and Department of Chemistry, University of Modena, Modena 41100, Italy, the ¶Laboratory of Structure-Function Biochemistry, Department of Chemistry, Kyusho University, Fukuoka, Japan, and the **Department of Pharmacology, Ankara University, Ankara 06339, Turkey*

**We converted Ser-207, located in helix 5 of the $\beta_2$-adrenergic receptor, into all other natural amino acids. To quantify receptor activation as a receptor number-independent parameter and directly related to $G_s$ activation, we expressed the mutants in a $G\alpha_s$-tethered form. GTP exchange in such constructs is restricted to the fused $\alpha$-subunit and is a linear function of the receptor concentration. Except S207R, all other mutants were expressed to a suitable level for investigation. All mutations reduced the binding affinities of the catechol agonists, epinephrine and isoproterenol, and the extent of reduction was unrelated to the residue ability to form hydrogen bonds. Instead, both enhancements and reductions of affinity were observed for the partial agonist halostachin and the antagonist pindolol. The mutations also enhanced and diminished ligand-induced receptor activation, but the effects were strictly ligand-specific. Polar residues such as Asp and His exalted the activation by full agonists but suppressed that induced by the partial agonists halostachin and dichloroisoproterenol. In contrast, hydrophobic residues such as Ile and Val augmented partial agonist activation. Only Ile and Lys produced a significant increase of constitutive activity. The effects on binding and activity were not correlated, nor did such parameters show any clear correlation with up to 78 descriptors of amino acid physicochemical properties. Our data question the idea that Ser-207 is exposed to the polar crevice in the unbound receptor. They also suggest that the active receptor form induced by a full agonist might be substantially different from that caused by constitutive activation.**

The cluster of serines, comprising Ser-203(5.42), Ser-204(5.43), and Ser-207(5.46), in H5 of the $\beta_2$-adrenergic receptor, is thought to be involved in both agonist binding and receptor activation (1–8). Initial site-directed mutagenesis studies identified Ser-204(5.43) and Ser-207(5.46) as the most likely putative docking sites for catecholic hydroxyl groups of adrenergic agonists (1, 2), although position 5.43 is not absolutely conserved like 5.42 and 5.46, within the subfamilies of catecholamine-binding GPCRs.[1] More recent work (3, 4) revealed that mutagenesis of Ser-203(5.42) can affect ligand binding and activity just like the other two serines and suggests that all three residues may be crucial for catecholamine interaction with the $\beta_2$AR. However, the question of how these residues may contribute to ligand-receptor interactions remains open.

Using a double alanine mutant in 5.43 and 5.46 positions (S204A,S207A) we noted that the simultaneous removal of the two residues appears to reduce the rather small constitutive activity of the $\beta_2$AR, suggesting that the presence of the serine motif in H5 might control the intrinsic equilibrium between active and inactive receptor forms (5). We also found that for each of the three residues the loss of binding affinity due to OH removal is inversely related to the number of additional interacting groups in the non-catecholic part of the catecholamine molecule (6, 7). This behavior suggests an "induced-fit" mechanism in catecholamine binding, such that initial contacts between ligand and receptor sub sites facilitate the establishment of the subsequent interactions. A similar scenario emerges from the analysis of catecholamine interaction with fluorophor-labeled $\beta_2$AR, where multistep kinetics was found to depend on the number of functional groups present in the catecholamine molecule (8). A stepwise mechanism for the conversion of the $\beta_2$AR into active form was also proposed to explain why the various functional groups in the catecholamine molecule contribute synergistically to ligand binding and receptor activation (9).

All such evidences, along with an increasing understanding on the role of SS*XX*S motifs in transmembrane helices orientation (10, 11) and interactions (12), indicate that the serine triad in H5 may play a vital role in the conformational motion of the $\beta_2$AR.

In this study, we have further investigated the contribution of H5 serines on ligand affinity and efficacy of the $\beta_2$AR. To scan a significant range of conformational perturbations and minimize the extent of receptor modification, we replaced a single residue by all other possible amino acids. Ser-207(5.46), the most intramembranous of the three serines, was targeted in this study.

* This work was supported in part by the Ministero dell'Istruzione dell'Università e della Ricerca (Italy) Grant Fondo Italiano per la Ricerca di Base RBA01XWSA_003 and by the Mombushu Foundation (Japan) for a visiting fellowship (to Y. C.). The costs of publication of this article were defrayed in part by the payment of page charges. This article must therefore be hereby marked "*advertisement*" in accordance with 18 U.S.C. Section 1734 solely to indicate this fact.

‖ Present address: Dept. of Biological Chemistry, Hokkaido University, Sapporo 060-0810, Japan.

‡‡ To whom correspondence should be addressed. Tel.: 39-064-990-2386; Fax: 39-064-938-7104; E-mail: tomcosta@iss.it.

[1] The abbreviations used are: GPCR, G protein-coupled receptor; H1–H7, helices 1–7; MAPE, (±)2-(methylamino)-1-phenyl-1-ethanol (or, halostachin); ISO, isoproterenol; EPI, epinephrine, PIN, pindolol; DCI, dichloroisoproterenol; MEI, maximal exchange index; BEI, basal exchange index; SCAM, substituted cysteine accessibility method; MD, molecular dynamics; $\beta_2$AR, $\beta_2$-adrenergic receptor; MTSEA, methanethiosulfonate ethylamine; GTPγS, guanosine 5′-3-*O*-(thio)triphosphate; CAM, constitutive active mutant.

To quantify ligand efficacy as the true intrinsic ability to drive receptor activation, without the confounding effects of changes in signaling stoichiometry, receptor trafficking, or interactions with additional effectors, all mutants were expressed as a functional receptor-G$\alpha_s$ fusion protein cassette. In such chimeric constructs the measurable GTP-exchange response only comes from the receptor-tethered $\alpha$-subunit (13, 14), and the forced 1:1 stoichiometry of receptor:G$\alpha$ expression makes maximal agonist stimulation a linear function of the fusion protein concentration. That corrects for the differences in expression levels. Although providing a somewhat reductive picture of the functional properties of the mutants, this approach can quantify efficacy with a precision comparable to binding affinity.

Our results suggest that the serine in position 5.46 might not be available for interaction with the catechol moiety of agonist by default, but become accessible as a consequence of conformational changes that follow initial interactions between ligand and receptor. Also, the analysis of the various functional phenotypes obtained by mutagenesis indicates that the constitutively active receptor form induced by mutagenesis might be similar to a receptor activated by partial agonist, but substantially different from the active form induced by the full agonist.

## EXPERIMENTAL PROCEDURES

*Materials*—All biochemicals, including nucleotide analogs, were from Sigma. Culture media and fetal calf serum were from Invitrogen. Methanethiosulfonate ethylamine (MTSEA, $CH_3SO_2$-$SCH_2CH_2NH_3^+$) was purchased from Toronto Research Chemicals, Inc. (Toronto, Ontario, Canada). Radiolabeled ligands and nucleotides were from PerkinElmer Life Sciences. Molecular biology kits and reagents were from Qiagen, Invitrogen, Stratagene, and New England Biolabs.

*Mutagenesis*—The preparation of full-length cDNAs encoding the $\beta_2$AR-G$\alpha_{sL}$ fusion protein was described previously (13). Site-specific mutagenesis was performed by a PCR-based strategy, using mismatched primers and *Pfu* DNA polymerase (Stratagene). The PCR products were digested with KpnI and EcoRV and subcloned into the pcDNA3 expression vector (Invitrogen) containing the cDNA encoding the human wild-type $\beta_2$AR-G$\alpha_s$ fusion protein. Recombinant clones were isolated, and the inserted mutations were confirmed by sequencing.

*Cell Culture, Transfection, and Membrane Preparation*—COS7 and HEK-293 cells were grown in Dulbecco's modified Eagle's medium Dulbecco's modified Eagle's medium supplemented with 10% (v/v) fetal calf serum, 100 units/ml penicillin G, and 100 $\mu$g/ml streptomycin sulfate, in a humidified atmosphere of 5% $CO_2$ at 37 °C. Transient transfections were performed by DEAE-dextran/chloroquine and calcium phosphate precipitation for COS7 and HEK-293 cells, respectively. Enriched plasma membranes from transfected cells were prepared as described previously (13) and stored frozen (as ≥2 mg/ml) at −80 °C.

*Receptor Binding Assays*—Were made in 1-ml reactions containing 50 mM Hepes-Tris, pH 7.4, 0.2 mM EGTA, 0.2 mM dithiothreitol, 5 mM $MgCl_2$, 10 mM leupeptin, 10 mM bestatin, 0.1 mg/ml bacitracin, 0.1% (w/v) bovine serum albumin, and suitable amounts of membrane proteins (0.5–2 $\mu$g). [$^{125}$I]Pindolol (50–100,000 cpm) was used as radiotracer. Receptor number ($B_{max}$) was computed from competition binding curves constructed using 12 log-spaced concentrations of unlabeled pindolol.

*Reaction with MTSEA*—MTSEA treatment was performed according to the procedure of Javitch *et al.* (15), with minor modifications. COS7 cells, plated in T25 flasks or 6-wells plates, were washed 48 h after transfection with phosphate-buffered saline, and incubated for 2 min at room temperature with freshly prepared MTSEA at the desired final concentrations. The reactions were stopped by aspiration, followed by two washes with ice-cold phosphate-buffered saline (the first containing 10 mM cysteine). Cell monolayers were then resuspended and homogenized by Polytron in binding buffer (50 mM Tris/HCl, 0.1% bovine serum albumin, pH 7.4), and incubated as quadruplicate aliquots in the presence of [$^3$H]CGP-12177 (100,000 cpm), plus and minus 1 $\mu$M pindolol, to evaluate nonspecific binding. Binding reactions lasted 60 min and were terminated by rapid filtration on GF/B glass fiber filters. The fractional binding due to the exposure to MTSEA was calculated as the ratio: specific binding after the MTSEA treatment/specific binding without the treatment.

*GTPase and Adenylyl Cyclase Stimulation*—The measurement of GTPase and adenylyl cyclase activities was done as described previously (13).

*GTP$\gamma$S binding*—[$^{35}$S]GTP$\gamma$S binding was determined in a 100-ml reaction mixture containing 50 mM Hepes-Tris, pH 7.4, 1 mM EGTA, 1 mM dithiothreitol, 100 mM NaCl, 5 mM $MgCl_2$, 1 nM [$^{35}$S]GTP$\gamma$S (~1200 Ci/mmol), 3 $\mu$M GDP, and 1–5 $\mu$g of membrane proteins, with or without the appropriate agonist. Samples were incubated 90 min at 20 °C, filtered onto GF/B (Packard Filterplate), and washed with ice-cold buffer (6–10 volumes) prior to scintillation counting on a microplate radioactivity reader (Packard Top Count). Specific binding (picomoles/mg of membrane protein) was computed by subtracting the binding measured in the presence of 10 $\mu$M GTP$\gamma$S. To measure maximal exchange indices (see "Data Analysis"), agonist concentrations were 100 $\mu$M (ISO, EPI, and DCI) and 1 mM (MAPE). To compare G protein activation across various mutants, membranes were prepared from sets of cells transfected with control pcDNA3 and vectors encoding wild-type and mutant constructs (from 5 up to 18 in each experiment). After protein determinations and the collection of aliquots for the analysis of receptor density (see $B_{max}$ above), GTP$\gamma$S binding (measured in quadruplicate) was determined for all membranes in the same experiment. Lower expressed mutants (Lys, Tyr, Asp, and Ile) were tested using 5 $\mu$g of protein, whereas 1 $\mu$g of proteins was used for all the others.

*Data analysis*—Apparent equilibrium dissociation constants ($K_d$) were calculated by non-linear fitting of the competition curves according to a four-parameter logistic equation, using the program ALLFIT (16). Maximal binding capacity ($B_{max}$) was calculated by fitting the binding curves with the program LIGAND (17). The apparent dissociation constants were converted to free energy changes, *i.e.* $\Delta G = -\ln(1/K_d)$, given as $RT$ units ($R$, gas constant; $T$, absolute temperature). The variation in free energy due to mutation, $\Delta\Delta G$, was calculated as the difference in binding energy between mutant and wild-type receptor, $\Delta\Delta G = \Delta G(mut) - \Delta G(wt)$. Energy values were computed experiment by experiment before taking averages, so that their variances reflect the true experimental error and are not amplified by the errors due the subtractions of averaged starting values.

The intrinsic activity of receptor mutants was evaluated by converting GTP$\gamma$S binding results (picomoles/mg) into two expression level-independent dimensionless indices. The enhancement of nucleotide binding (see "Results" and Fig. 1, *C* and *D*) is a linear function of the membrane concentration of fusion protein both in the absence and presence of ligand. Because receptor number = picomoles of the tethered $G_s$, data were divided by the $B_{max}$ (picomoles/mg) measured in the corresponding membranes as in the following equations: basal exchange index (BEI) = (GTP$\gamma$S binding in receptor transfected cells − GTP$\gamma$S binding in pcDNA3 transfected cells)/$B_{max}$. Maximal exchange index (MEI) = (GTP$\gamma$S binding plus agonist − GTP$\gamma$S binding minus agonist)/$B_{max}$. The first index represents the basal binding of the transfected construct and is significantly enhanced if a mutation increases receptor constitutive activity. The second measures the net ligand-induced stimulation and represents the intrinsic activity (efficacy) of the ligand, when recorded at a saturating concentration of agonist. Data were averaged from many transfection experiments, and the standard deviations of their differences were calculated from the sum of the variances of the two variables.

*Comparative Modeling of the $\beta_2$AR and MD Simulations*—A molecular model of the human $\beta_2$AR, truncated at Ser-345, was built by comparative modeling, by means of the MODELLER program (18), using a modified version of the 2.2-Å x-ray crystal structure of rhodopsin as a template (19).

The general strategy used to select the final structure involved a multistep optimization and refinement process, which is described in detail elsewhere (20). Briefly, the following steps were carried out: (i) Each of five different templates was used to generate 50 models by randomizing the model coordinates through a random number uniformly distributed in the interval −4/+4 Å. Among the 250 models thus obtained, the three showing the lowest violations of spatial restraints and the highest 3D-Profile scores (Protein Health module in the QUANTA 2000 package (www.accelrys.com)) were selected. In the template used to achieve these models, amino acids 228–245 (third intracellular loop) were replaced with the corresponding loop extracted from the computational model of the $\alpha_{1b}$AR (21), and Q184,C185 (second intracellular loop) were deleted. In addition to the disulfide bridge Cys-106(3.25)–Cys-191, homologous to that present in rhodopsin, a second bridge was also imposed ("special patches" subroutine) between Cys-184 and Cys-190, in accordance with experimental data (22). (ii) The selected models, completed by the addition of polar hydrogens, were subjected to automatic and manual rotation of the side-chain torsion

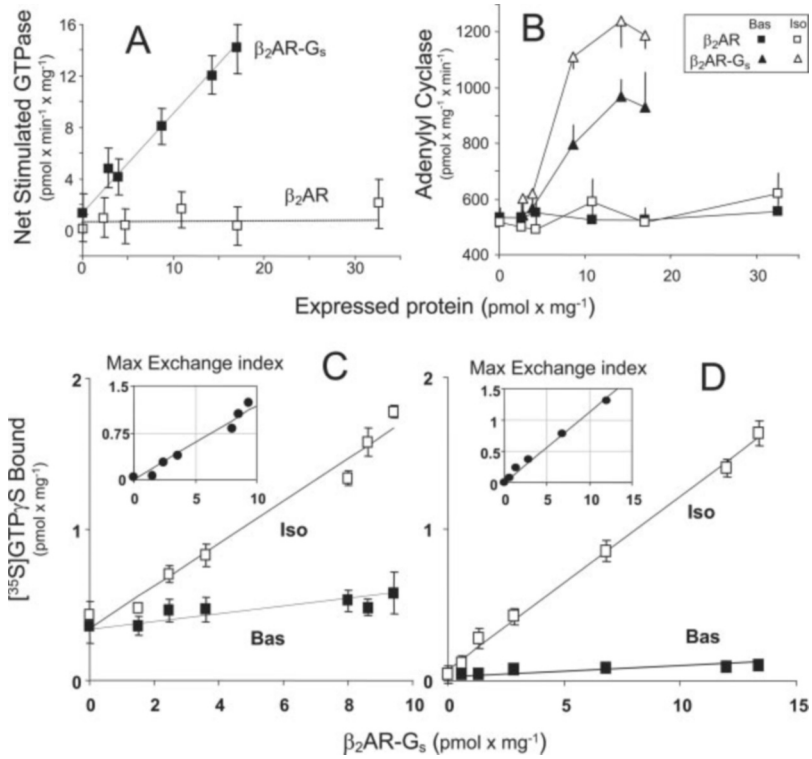


FIG. 1. **"Fusion-specificity" of the GTP exchange signal and its linearity with the expression level of the construct.** *Upper panels*, membranes were prepared from COS cells transfected with a constant amount (2 $\mu$g) of a mix consisting of reciprocally changing concentrations of empty pcDNA3 and vector expressing either wild-type $\beta_2$AR or the fusion protein $\beta_2$AR-G$\alpha_{sL}$. The net GTPase activity (difference between the presence and absence of 100 $\mu$M ISO) (*A*) and adenylyl cyclase activity (*B*) are plotted as a function of the receptor concentration measured in the membranes. Data are means (±S.E.) of triplicate determinations. *Lower panels*, membranes prepared from COS7 (*C*) or HEK-293 (*D*) cells, transfected with increasing amounts of fusion construct, as described above. Specific GTPγS binding in the absence (*Bas*) or presence of ISO is plotted *versus* receptor concentrations. The best fitting lines were computed by linear regression. The net agonist-stimulated binding (to assess maximal exchange index) is replotted in the *insets* of the two graphs. The slopes (MEI) obtained by linear regression analysis are: 0.12 ± 0.005 in COS7 cells (*C*) and 0.11 ± 0.002 in HEK-293 cells (*D*).

angles, when in non-allowed conformations. (iii) Next, the models were submitted to extensive energy minimization and molecular dynamics (MD) simulation procedures, essentially as described previously (20), except that an implicit membrane-water model (23) (IMM1), recently implemented in CHARMM (24), was employed (with the adjustable parameter "*a*" and the non-polar core thickness set as 0.85 and 32 Å, respectively). (iv) The final input structure, selected on the basis of structural quality checks and degree of similarity to rhodopsin structure, was finally subjected to 1 ns of equilibrated MD simulation. The structures averaged over 1 ns as well as over the first and last 500 ps were considered for the structural analysis.

*Numbering of $\beta_2$AR Residues*—Residues are numbered with two figures. The first is the position in the human $\beta_2$AR sequence. The second, (in parenthesis), is the position relative to the most conserved residue of the helix in the macro alignment of class A GPCRs (25).

## RESULTS

*Validity of the Receptor-$G_s$ Fusion System for the Study of the Effect of Receptor Mutations*—As shown in Fig. 1*A*, we used membranes from COS cells, transiently transfected with increasing amounts of either $G_s$-fused or wild-type receptor vectors to evaluate the fusion protein "specificity" of the guanine nucleotide exchange signal. Net agonist-stimulated GTPase activity and GTPγS binding (not shown) increased with the enhanced expression of fused receptor, but remained close to zero even at very high levels of non-fused receptor expression. This confirms that no significant contribution from the interaction of the receptor with endogenous $G_s$ can be detected in such read-out (13). Adenylyl cyclase activity in the same membranes displayed a different pattern. The increased expression of fusion protein resulted in a large enhancement of basal activity, which reflects the increase of G$\alpha_s$ concentration, rather than ligand-independent receptor activity, because identical effects were observed when expressing a fusion protein made between opioid-δ receptor and G$\alpha_s$ (not shown). Moreover, ligand-induced enhancement of adenylyl cyclase was not linear and reached saturation at relatively low levels of fusion protein expression (Fig. 1*B*). Thus, the tethered receptor-G$\alpha$ system provide quantitative information on ligand-induced receptor activation only if the measured end-point is direct G protein activation, not effector-mediated signaling.

The binding of GTPγS increased linearly with the number of adrenergic binding sites both in the presence and absence and of a maximal agonist concentration (Fig. 1, *C* and *D*). The net difference was a linear function of fusion protein expression (Fig. 1, *C* and *D*, *insets*) with zero intercept and a dimensionless slope, which represents a quantitative estimate of the agonist power to activate the system (intrinsic activity). This value, called maximal exchange index (MEI), is independent of expression level. Thus, by taking the ratio, net picomoles/mg of stimulated GTPγS binding *versus* net picomoles/mg of expressed receptor, we can compare the ability of ligands to maximally activate receptors across membranes expressing different levels of mutants. The enhancement of [$^{35}$S]GTPγS binding was insensitive to pertussis toxin, but markedly reduced by cholera toxin treatment (data not shown), indicating lack of interferences from endogenous $G_{i/o}$ proteins. In addition, the typical pattern of ligand intrinsic activities for the $\beta_2$AR was maintained in the fusion protein construct. In fact, isoproterenol (ISO) and epinephrine (EPI) displayed greater intrinsic activity than dobutamine and halostachin (MAPE), whereas dichloroisoproterenol (DCI) behaved as a weak partial agonist (Fig. 2*A*).

*Ligand Binding Affinity for the Receptor Mutants*—To evaluate the binding affinity of $\beta_2$AR-G$\alpha_s$ mutants correctly, the recombinant protein must be expressed to a level at least 10-fold greater than that of the endogenous $\beta_2$AR in the host cells (which, in COS cell lines, can range between 0.05 and 0.2 pmol/mg of membrane proteins). All residue substitutions, but Arg-207, resulted in receptors that met such criterion. The S207R mutant was thus excluded from the rest of the study. Fig. 2*B* reports a summary of the expression levels recorded through this investigation (data are normalized to the level of expression of the wild-type construct, which was always determined in each experiment). The differences of expression among mutations ranged from 0.3- (S207K) to 2.1-fold (S207G) the wild-type. Whether such diversity may reflect differences in receptor stability or folding efficiency was not investigated in this study.

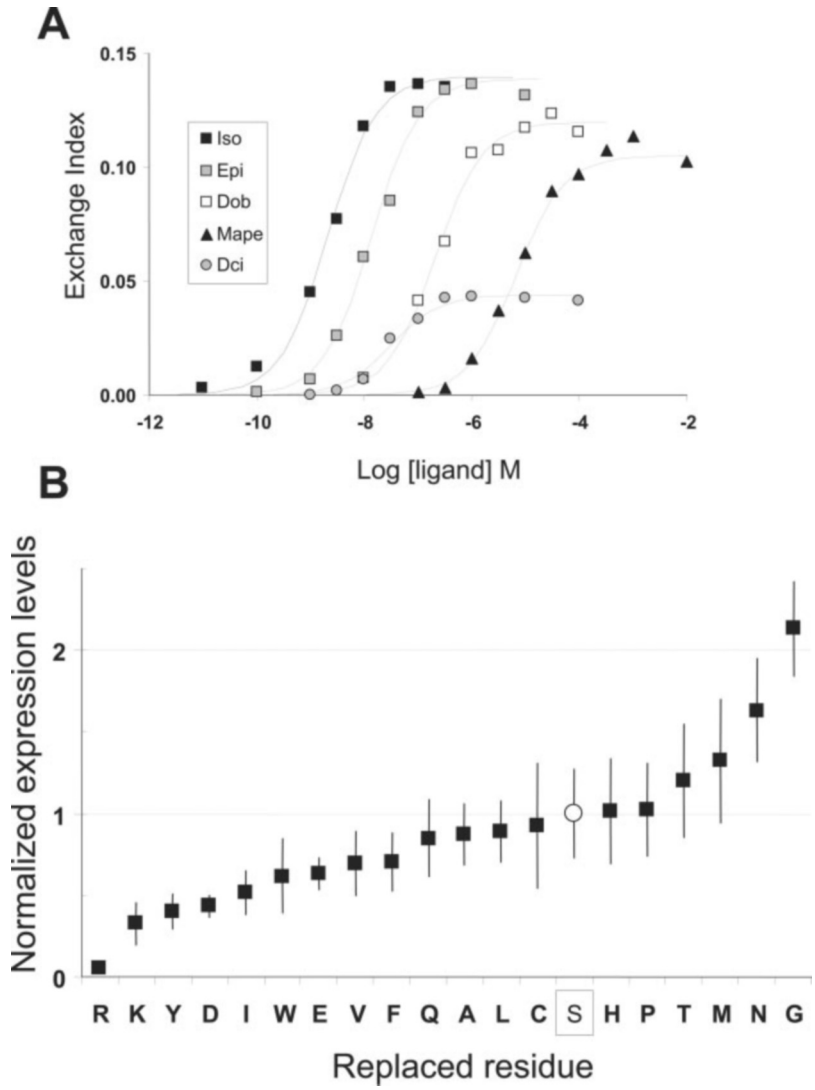


FIG. 2. **Intrinsic activities at receptor-tethered $G_s$ and expression levels of mutant chimeras.** *A*, specific GTPγS binding in membranes prepared from COS cells transfected with wild-type $\beta_2$AR-G$\alpha_s$ and incubated with various concentrations of adrenergic agonists, as indicated. Data were converted into exchange index (*i.e.* agonist-stimulated binding/$B_{max}$, see "Experimental Procedures") and fitted with ALLFIT (*solid lines*) to compute the maximal effect of each ligand: *Iso*, 0.139 (±0.03); *Epi*, 0.138 (±0.04); dobutamine (*Dob*), 0.12 (±0.03); *Mape*, 0.10 (±0.02); *DCI*, 0.044 (±0.015). The rank order of relative intrinsic activities (*Iso* ≅ *Epi* > *Dob* > *Mape* > *DCI*) correspond to that commonly found for non-fused receptor stimulation of adenylyl cyclase. *B*, relative expression values of mutagenized constructs ($B_{maxmut}$/$B_{maxwild\text{-}type}$) measured after transfections in both COS7 and HEK-293. Data are averages (±S.D.) of 8–6 independent experiments (except for Arg-207, with $n = 3$). The mutations are shown on the *x*-axis as single letter notations. The average $B_{max}$ for the wild-type (*boxed S* = 1) is 9.2 (±2.2) pmol × $mg^{-1}$.

The binding affinities of the ligands, ISO, EPI, MAPE, and pindolol (PIN) for all mutants are listed as logarithms of the apparent dissociation constants in Table I. To visualize the relative potency of each mutated residue to shift binding affinity with respect to wild-type receptor, we also plotted the data as ΔΔG changes (*i.e.* ΔG mutant minus ΔG wild-type) for each ligand, ranked according to the magnitude of the residue effect (Fig. 3). The most prominent finding of this analysis is that the changes in binding affinity produced by the mutations are ligand-specific.

EPI and ISO, both full agonists with catechol rings, displayed the closest patterns. All mutations produced a loss of binding affinity for such ligands, but the extent of reduction varied greatly. Residues such as Glu, Pro, and Gln produced the largest diminutions (with some differences between EPI and ISO in the relative effects of Pro and Gln). Thr, His, and Gly produced the smallest decrease. Other than noting that Thr (the most conservative replacement for the wild-type Ser) produced the smallest decrease of binding affinity, there was no obvious relationship between the residue ability to be H-bond donor/acceptor and its effect on binding affinity.

The changes of binding affinity for the non-catecholic partial agonist MAPE was quite different from that observed for the two catecholamines. Both enhancements and reductions in binding affinity were observed, and the largest changes were not produced by the same residues that mostly affected catecholamines. The aliphatic residues Val and Ile maximally enhanced binding affinity, whereas Asn, Gln, and Lys produced marked reductions. Unlike that of catecholamines, the affinity of MAPE was only slightly changed by Glu and Pro replacements.

A still different pattern was observed for the antagonist PIN. Many residues produced little change or slight increases of binding affinity, but significant diminutions were caused by Lys and Pro mutations (Fig. 3).

*Shifts of Ligand-induced Receptor Activation*—To measure how mutations altered the intrinsic ability of ligands to activate the receptor, we determined maximal exchange indexes (see "Experimental Procedures") for EPI, ISO, MAPE, and the weak partial agonist dichloroisoproterenol (DCI), in numerous transfection experiments performed both in COS7 and HEK-293. The data, normalized with respect to the activation observed in the wild-type construct, are shown in Fig. 4.

ISO and EPI were again affected in a similar fashion. Many residues caused loss of ligand-induced activation, most effectively Leu, which produced an essentially inactive receptor, and, next in rank, Met, Pro, Asn, and Glu, all of which resulted in ≤20% of the activation observed in wild-type. Surprisingly, some residues improved agonist-induced receptor activation, particularly Asp and His, the latter resulting in up to 2-fold enhancement of agonist-mediated $G_s$ activation. As observed for binding affinity, no obvious relationship between amino acid property and effect on activation is evident. For example, His and Asp, which bear opposite charges, can both potentiate

TABLE I
*Apparent ligand binding affinities of receptor mutants*

| Residue in 207 | $\text{Log}_{10}(K_d)$ M | | | | | | | |
|---|---|---|---|---|---|---|---|---|
| | Isoproterenol | | Epinephrine | | MAPE | | Pindolol | |
| | Mean (±S.E.) | *n* | Mean (±S.E.) | *n* | Mean (±S.E.) | *n* | Mean (±S.E.) | *n* |
| Ala | −5.58 (0.11) | 5 | −4.65 (0.32) | 3 | −4.36 (0.25) | 3 | −9.70 (0.05) | 8 |
| Cys | −5.52 (0.11) | 4 | −4.38 (0.23) | 3 | −4.19 (0.17) | 3 | −9.67 (0.04) | 7 |
| Asp | −5.95 (0.03) | 6 | −5.01 (0.17) | 3 | −4.19 (0.02) | 3 | −9.04 (0.07) | 10 |
| Glu | −4.98 (0.02) | 6 | −3.97 (0.01) | 3 | −3.91 (0.01) | 3 | −8.73 (0.08) | 10 |
| Phe | −6.00 (0.03) | 6 | −5.02 (0.24) | 3 | −4.27 (0.12) | 3 | −9.34 (0.06) | 10 |
| Gly | −6.15 (0.09) | 3 | −5.16 (0.25) | 3 | −3.85 (0.15) | 3 | −9.06 (0.04) | 6 |
| His | −6.20 (0.05) | 6 | −5.32 (0.28) | 3 | −3.86 (0.14) | 3 | −9.50 (0.03) | 10 |
| Ile | −5.22 (0.08) | 3 | −4.31 (0.02) | 4 | −4.91 (0.09) | 4 | −9.40 (0.02) | 5 |
| Lys | −4.89 (0.07) | 3 | −4.12 (0.09) | 3 | −3.64 (0.06) | 3 | −8.30 (0.04) | 3 |
| Leu | −5.86 (0.08) | 3 | −4.90 (0.24) | 3 | −3.96 (0.13) | 3 | −9.47 (0.03) | 6 |
| Met | −5.54 (0.10) | 3 | −4.37 (0.15) | 3 | −3.81 (0.14) | 3 | −9.41 (0.04) | 6 |
| N | −5.59 (0.05) | 6 | −4.33 (0.28) | 3 | −3.44 (0.18) | 3 | −9.30 (0.02) | 10 |
| Pro | −4.95 (0.10) | 3 | −4.00 (0.21) | 3 | −3.94 (0.08) | 3 | −8.03 (0.11) | 3 |
| Gln | −5.42 (0.10) | 6 | −3.88 (0.39) | 3 | −3.47 (0.31) | 3 | −9.69 (0.05) | 10 |
| Ser | −6.81 (0.10) | 7 | −6.42 (0.16) | 4 | −4.14 (0.06) | 4 | −9.41 (0.03) | 10 |
| Thr | −6.39 (0.07) | 5 | −6.03 (0.21) | 3 | −4.43 (0.04) | 3 | −8.79 (0.03) | 8 |
| Val | −5.45 (0.09) | 3 | −4.35 (0.22) | 3 | −4.98 (0.11) | 3 | −9.51 (0.03) | 6 |
| Trp | −5.67 (0.07) | 3 | −4.91 (0.12) | 3 | −4.13 (0.07) | 3 | −8.73 (0.02) | 6 |
| Tyr | −5.56 (0.05) | 6 | −4.88 (0.11) | 3 | −4.66 (0.03) | 3 | −9.17 (0.03) | 10 |

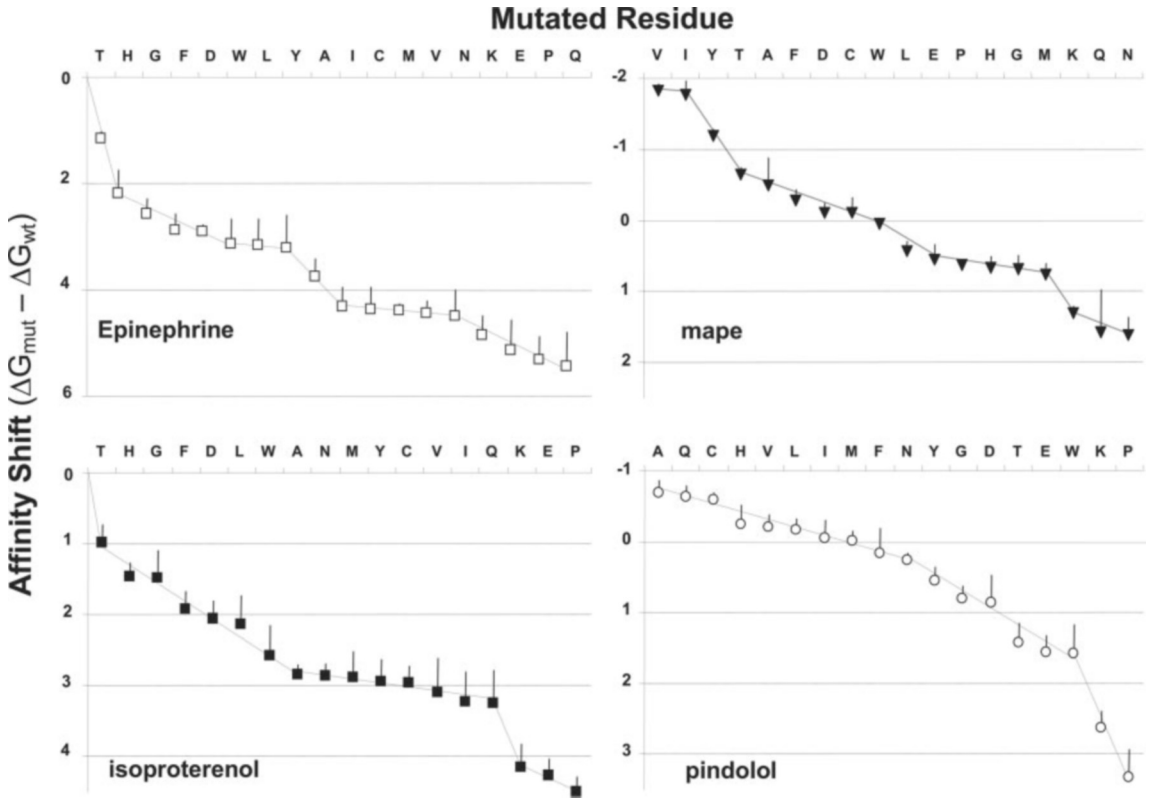


FIG. 3. **Ligand affinity shifts caused by the mutations.** ΔΔG values (calculated as described under "Experimental Procedures") are means (±S.E.) of 4–10 independent experiments. Data are sorted from the lowest to the highest value in each plot, making the rank order of the mutations different for each *x*-axis. Note that negative values denote increase, whereas positive values decrease, of binding affinity.

receptor activation, whereas Glu (a conserved replacement for Asp) results in marked loss of activation. Likewise, the closely related isomers Ile and Leu produced divergent effects, improving and abolishing, respectively, catecholamine-induced maximal activation.

The pattern of effects on the receptor activation induced by MAPE displayed both similarities and differences with respect to catecholamines. Marked reductions, roughly similar to those produced on the activation index of EPI and ISO, were caused by Asn, Leu, Glu, and Tyr. Also Pro diminished activation, but to a much smaller extent than for catecholamines. The two charged residues His and Asp did not enhance, but significantly reduced MAPE-induced activation. Also at variance with catecholamines, aliphatic residues such as Val, Ile, and to a lesser extent Ala, were the most effective in generating improvement of MAPE-induced activation compared with wild-type receptor (Fig. 4).

Although the overall pattern of effects on the activation induced by DCI resembles more closely that observed for MAPE than for catecholamines, a number of DCI-specific changes were noted. Val and Ala, but also Lys, produced enhancement of activation, whereas Ile did little or nothing. As observed for MAPE, the charged residues His and Asp did not enhance, but diminished DCI-induced activation (Fig. 4).

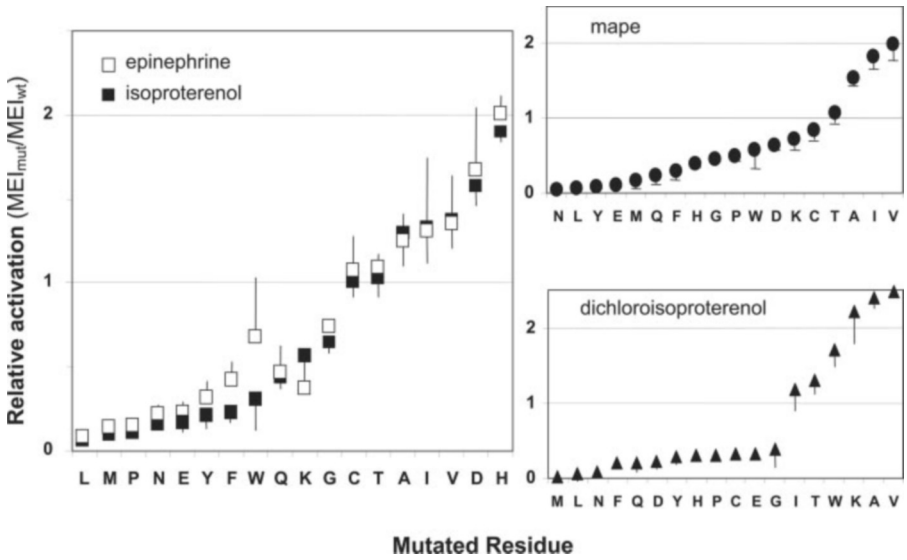


FIG. 4. **Shifts of ligand-induced maximal activation caused by the mutations.** The maximal exchange index (MEI) (calculated from GTPγS stimulation data as described under "Experimental Procedures") of each mutation was normalized to the wild-type value ($MEI_{mut}/MEI_{wild\text{-}type}$), which was assayed in every experiment. Data are means (±S.E.) of independent experiments averaged from both COS7 and HEK-293 transfections. Given the similarity, Iso and Epi data are shown in the same plot. The average values for the wild-type chimera are: ISO, 0.144 (±0.02, $n$ = 10); EPI, 0.13 (±0.03, $n$ = 4); MAPE, 0.11 (±0.03, $n$ = 6); and DCI, 0.05 (±0.008, $n$ = 4).

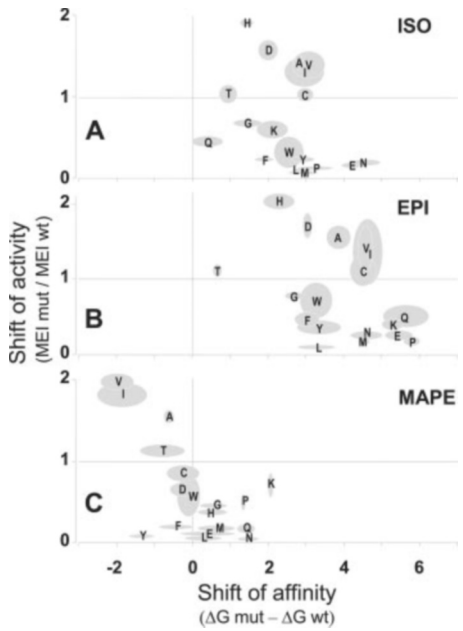


FIG. 5. **Relationships between the effects of the mutations on binding affinity and activity of three adrenergic ligands.** The data presented in Figs. 3 and 4 were replotted to show the relation between shift of affinity and shift of maximal activation induced by the mutations for the three ligands indicated in the graphs. The position of each data point is labeled by the letter corresponding to the mutant residue. *Shaded contours* were traced around the *y*- and *x*-axis *error bars*. Linear regression of the data gave a significant correlation only for MAPE (correlation coefficient: 0.62, $p$ = 0.005). If the data points corresponding to Val and Ile mutants are omitted from calculations, the correlation was no longer significant (correlation coefficient: 0.29, $p$ = 0.26).

*Relation between Affinity and Activity, and Correlations with Physicochemical Descriptors of Amino Acids*—The relationship between shifts in ligand-induced activation and shifts in binding affinity produced by the 18 mutations for the three ligands EPI, ISO, and MAPE is shown in Fig. 5. As evident from the dispersion of the data points, no significant correlation between binding and activation was found for ISO or EPI (Fig. 5, *A* and *B*). A weak ($r$ = 0.62), albeit statistically significant ($p < 0.01$), correlation coefficient was measured for MAPE (Fig. 5*C*). We note, however, that the significance of such correlation is critically dependent on the two residues Val and Ile, which for MAPE enhance both binding affinity and G protein activation. Their omission from the data set abolished the significance of the correlation.

The plots in Fig. 5 also serve as a "fingerprint" of the ligand-specific manner by which the series of point mutations in position 5.46 alter receptor properties. Apart from the obvious difference between MAPE and the two catecholamines, subtle divergences between ISO and EPI can also be appreciated. For example residues such as Gln, Pro, and Lys affect binding and activity differently for the two ligands.

We also searched possible relationships between the effects on binding/activity of the studied ligands and the chemical properties of the replaced amino acids. Up to 78 compilations of physicochemical properties of natural amino acids were considered, including hydrophobicity parameters, size, volume and surface area descriptors, solvation properties, $R$ values, polarity, and polarizability indices (26). Correlations were analyzed between all the amino acid descriptors and the receptor functional data presented above, (comprising the effect of residues on the shifts of affinity and activity for all the studied ligands, and the changes in receptor expression). None of the estimated correlation coefficients exceeded a value of 0.7. However, some correlations were statistically significant. An extract of the correlation matrix including coefficients reaching the 99% probability level is reported in Table II.

The shift of MAPE affinity was correlated with several hydrophobicity scales, and the shift in MAPE-mediated receptor activation with the propensity of the residue to be buried in a folded protein. Thus the hydrophobicity of the side chain may be a contributing component for the effects of the mutations on the interaction MAPE/receptor but plays no role for the other ligands. There were also negative correlations between changes in receptor expression and several measures of residue size, such as bulkiness, surface area, molecular, and Van der Waals volumes, indicating that the size of residue 207(5.46) disturbs either receptor folding or stability, which is more likely for a residue holding an inter-helical position. The change in receptor expression levels, however, did not correlate with any of the other receptor binding and functional parameters, which confirms that the determination of such properties is independent of the differences in the membrane concentration of the expressed constructs.

Finally, significant correlations were found between the shift in binding affinity of catecholamines and some amino acid chromatographic properties, related to the propensity to be eluted from silica or cellulose by acidic alcohol:water mixtures (Table II). Although of unclear significance, it is intriguing to

TABLE II
*Computed correlation coefficients between amino acids descriptors and mutations effects*

| I.D. | Descriptor | Effects of mutations | | | | | | | | |
|---|---|---|---|---|---|---|---|---|---|---|
| | | ΔΔG | | | | Shift of activity | | | | $B_{max}$ |
| | | *iso* | *epi* | *mape* | *pin* | *iso* | *epi* | *mape* | *dci* | |
| Asn-26 | Kyte and Doolittle hydropathy indices (26, and references therein) | NS[a] | NS | **−0.64**[b] | NS | NS | NS | 0.50[c] | NS | NS |
| CH | Chothia hydrophobicity scale (37) | NS | NS | **−0.63**[b] | NS | NS | NS | NS | NS | NS |
| Glu | Eisemberg hydrophobicity scale (38) | NS | NS | **−0.64**[b] | NS | NS | NS | NS | NS | NS |
| Asn-29 | Average surrounding hydrophobicity (39) | NS | NS | **−0.67**[b] | NS | NS | NS | NS | NS | NS |
| Ala-5 | Average solvent accessible area (folded) (26, and references therein) | NS | NS | 0.52[c] | **0.62**[b] | NS | NS | NS | NS | NS |
| Pro-70 | Proportion of residues 100% buried (37) | NS | NS | NS | NS | NS | NS | **0.61**[b] | NS | NS |
| Ala-7 | Bulkiness (26, and references therein) | NS | NS | NS | NS | NS | NS | NS | NS | **−0.61**[b] |
| Pro-3 | Molecular volume (40) | NS | NS | NS | NS | NS | NS | NS | NS | **−0.60**[b] |
| SA | Residue surface area (37) | NS | NS | NS | NS | NS | NS | NS | NS | **−0.62**[b] |
| RV | Residue volume (41) | NS | NS | NS | NS | NS | NS | NS | NS | **−0.60**[b] |
| Pro-100 | Van der Waals volume (42) | NS | NS | NS | NS | NS | NS | NS | NS | **−0.60**[b] |
| Asn-1 | −ΔG transfer ethanol/water (*kcal/mol*) (26, and references therein) | NS | NS | −0.58[c] | NS | NS | NS | NS | NS | **−0.66**[b] |
| AAC3 | Amino acid chromatographic properties (26, and references therein) | 0.61[c] | **0.70**[b] | NS | NS | NS | −0.52[c] | NS | NS | NS |
| AAC4 | | 0.62[c] | **0.70**[b] | NS | NS | −0.52[c] | −0.53[c] | NS | NS | NS |
| AAC11 | | 0.58[c] | **0.62**[b] | NS | NS | −0.50[c] | −0.52[c] | NS | NS | NS |
| AAC14 | | 0.54[c] | **0.61**[b] | NS | NS | NS | NS | NS | NS | NS |
| AAC19 | | 0.58[c] | **0.60**[b] | NS | NS | NS | NS | NS | NS | NS |

[a] NS (not significant).
[b] $p < 0.01$ (two-tailed tests).
[c] $p < 0.05$ (two-tailed tests).

find that only the affinity shift for catecholic ligands shows such a relationship.

*Changes of Receptor Constitutive Activity*—When increasing levels of a fusion protein are expressed in the membrane, there must be elevation of basal nucleotide binding due to the rising concentration of the tethered Gα-subunit, regardless of whether the receptor does or does not have constitutive activity. Therefore, the net difference of basal GTPγS binding between transfected and non-transfected cells (a good measure of the level of ligand-independent activity for non-fused receptors) is not as useful in the case of fusion proteins. It is still possible, however, to compare the basal exchange index of each mutant with that of wild-type construct, to spot mutations causing significant enhancement of constitutive activation. Given the high background levels of GTPγS binding activity in COS7 cells, we averaged basal exchange indices only from transfection experiments made in HEK-293 cells (Fig. 6). The experimental error was still large enough to prevent the identification of mutations that may diminish constitutive activity or to allow a reliable quantification of the rank order of potency in enhancing it. Yet, a few mutants with clear-cut enhancements of constitutive activity were found. The Ile-207 mutant, displaying the highest level of ligand-independent activity, was further characterized.

A $G\alpha_s$-tethered version of the original $\beta_2$AR constitutive active mutant (CAM), which carries four amino acid replacements in the C-terminal portion of the 3d intracellular loop (27), was used as reference. The extent of activation of S207I was roughly 60–70% that of the CAM mutation when the two receptors were examined in paired transfections (Fig. 7*A*). In both receptors, we also assessed the degree of exposure of Cys-285 to a membrane-impermeant methanethiosulfonate analog, to evaluate the degree of conformational change induced by constitutive activation (15). The extent of MTSEA reactivity in S207I was about 50% that of CAM (Fig. 7*B*). Thus, both functional and conformational evidences indicate that Ile-207 enhance the constitutive activity of the receptor, to an extent ranging 0.5- to 0.7-fold that produced by multiple mutations of the third intracellular loop.

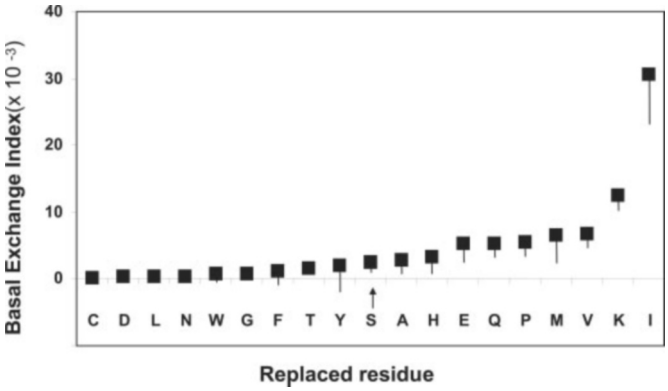


FIG. 6. **Effect of the mutations on basal exchange index.** Basal exchange indices (BEI) averaged from GTPγS binding measured in membranes from transfected HEK-293 cells. Data are means (±S.E.) of three and four independent experiments.

*Changes of Ligand Intrinsic Activity*—Mutations that affect differently the activation by catecholic and non-catecholic ligands may change the pattern of ligand efficacies for the receptor. We searched a single parameter that could accurately rank residues for their power to induce switches of efficacy. A good descriptor proved to be the net difference in normalized maximal exchange indices between pairs of ligands. Near-to-zero values indicate no change, whereas positive or negative values denote a switch of intrinsic activity in favor, respectively, of the first or the second ligand of the examined pair. Such differences between EPI and ISO were close to 0 for all residues (Fig. 8*A*), demonstrating that none of the 18 mutations substantially alter the relative power of the 2 catecholamines (both full agonists) to activate the receptor. Thus, either can be equivalently used to analyze the difference with the other ligands.

MEI differences between EPI *versus* MAPE (Fig. 8*B*) and EPI *versus* DCI (Fig. 8*C*), identify a number of mutants in which switches of maximal activation are evident. Asp and His

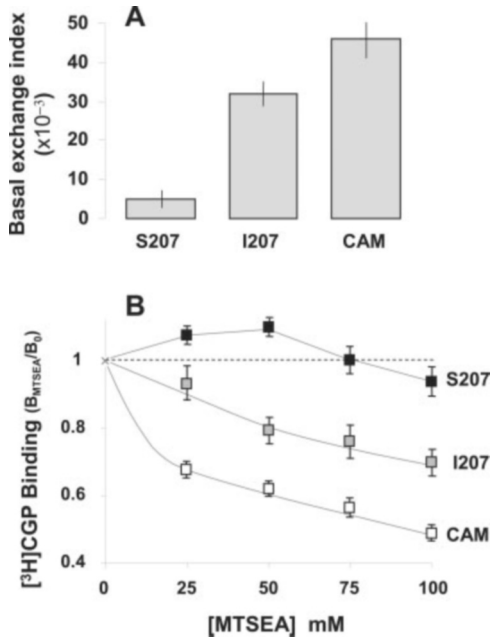


FIG. 7. **Comparison of the enhancement of constitutive activity induced by S207I and the CAM mutants.** *A*, HEK-293 cells were transfected with wild-type (*S207*) and two constitutively active mutant chimeras (*I207* and *CAM*). The concentration of expressed proteins ($B_{max}$) and specific GTP$\gamma$S binding were measured in plasma membranes and used to calculate basal exchange indices. Data are means (±S.E.) of three independent experiments. *B*, COS7 cells transfected with the same proteins were used to determine the degree of antagonist binding inhibition following exposure to MTSEA as described under "Experimental Procedures." Data are means (±S.E.) of four independent experiments.

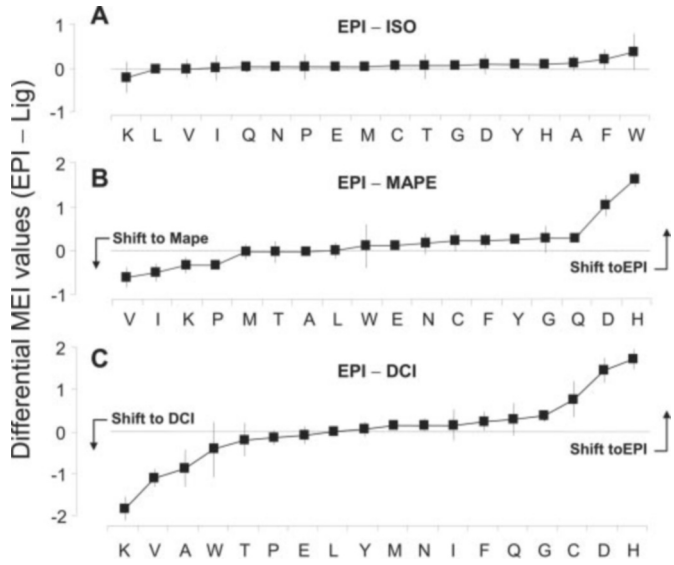


FIG. 8. **Opposite shifts of maximal ligand-induced activation produced by the mutations.** The net difference in normalized maximal exchange index (MEI, see Fig. 4) between EPI and ISO (*A*), EPI and MAPE (*B*), or EPI and DCI (*C*), were plotted over the replaced residues. Data are sorted from the lowest to the highest value in each graph. Positive values indicate a shift of maximal activation in favor of EPI, whereas negative values indicate a shift toward the activation induced by the subtracted ligand. Note that the difference, EPI − ISO, is near to zero for all ligands, thus essentially identical values are obtained when MEI values for ISO are used to take the differences (not shown). Data were computed from the averages shown in Fig. 5, and the *error bars* are approximate standard deviations calculated from the sum of the variances of the two means.

enhanced the maximal stimulations induced by catecholamine and concurrently reduced those induced by both MAPE and DCI, indicating that such receptors have lost the ability to respond to partial agonists. In contrast, Ile, Val, Lys, and Ala caused a somewhat opposite switch, by enhancing the effect of the partial agonists compared with the catecholamines. While Lys and Val enhanced the stimulation of both DCI and MAPE, Ala and Ile only affected the first and the second, respectively (Fig. 8, *B* and *C*).

Concentration response curves for ligand-induced stimulation of GTP$\gamma$S binding by EPI, MAPE, and DCI were compared in the wild-type receptor and in the five mutants visualized in such analysis, Asp, His, Ile, Val, and Lys. The data, normalized to the effect produced by 100 mM ISO (Fig. 9*A*), confirm that in this subset of mutations there are extensive changes in the pattern of ligand efficacies.

In Asp and His mutants the relative intrinsic activity of MAPE (0.7–0.8 in wild-type) was reduced to 0.2 and 0.12, respectively, and that of the weaker partial agonist DCI (0.3–0.4 in wild-type), to $< 0.04$. Consequently, DCI became a pure competitive antagonist in the His mutant, as indicated by its ability to produce a parallel shift to the concentration-response curve for ISO (Fig. 9*B*). Such receptors are hyperactivated by full agonists and poorly activated by partial agonists.

In contrast, the aliphatic residues Ile and Val caused an inversion in the intrinsic activity of adrenergic ligands. The relative effect of MAPE was raised to 1.3 and 1.7 by Ile and Val, respectively, which makes this ligand the full agonist and catecholamines only partial agonists in such receptors. Val replacement also greatly enhanced the relative intrinsic activity of DCI (0.84 relative to ISO), but the Ile mutation did not (0.19). A similar, yet not identical, phenotype was generated by the Lys mutation. In this receptor, the intrinsic activities of DCI and MAPE were raised to the same level of ISO and EPI, so that all ligands appear as equally effective full agonists (Fig. 9*A*).

*Study of H5 Serines Orientation in Wild-type $\beta_2$AR by SCAM and Computational Modeling*—We used three $\beta_2$AR mutants carrying single Cys substitutions of the serines in H5 (7) to evaluate the relative accessibility of the residues by the substituted cysteine accessibility method (28). Fig. 10*A* shows that MTSEA at micromolar concentrations efficiently blocked ligand binding for S203C and S204C mutants, but up to 1 mM did nothing for S207C where a small 20% inhibition was only observed at 5 mM. This indicates that the residue 5.46 is far less exposed than the others to the polar core of the receptor.

Results of molecular modeling of the $\beta_2$AR over a rhodopsin template followed by extended MD simulations were in partial agreement with such findings. In the averaged structure, which is representative of the most recurrent configurations collected in this study (Fig. 10*B*), Ser-203(5.42) was clearly exposed toward the binding crevice, whereas Ser-207(5.46) pointed toward H3 at H-bond compatible distance from Thr-118(3.37). However, Ser-204(5.43) also displayed, on average, an inter-helical orientation, pointing toward H6, where it might interact with Asn-293(6.55). Interestingly, the analysis of the different MD trajectories generated in this study reveals that the stretch of residues 202–212 (comprising the serine cluster) is highly dynamic. Bulge-like deformations and local unwinding in this area were often observed and made S5.43 more oriented *versus* the binding crevice, whereas S5.46 remained inter-helical. Such a configuration, which is infrequent in the empty receptor, became more common in the EPI-bound form (results not shown). It is thus possible that the topology of S5.43 is altered by MTSEA entry, possibly via an interaction of its amino-tail with Asp-113(3.32). That could account for the discrepancy between SCAM results and the empty receptor configuration.

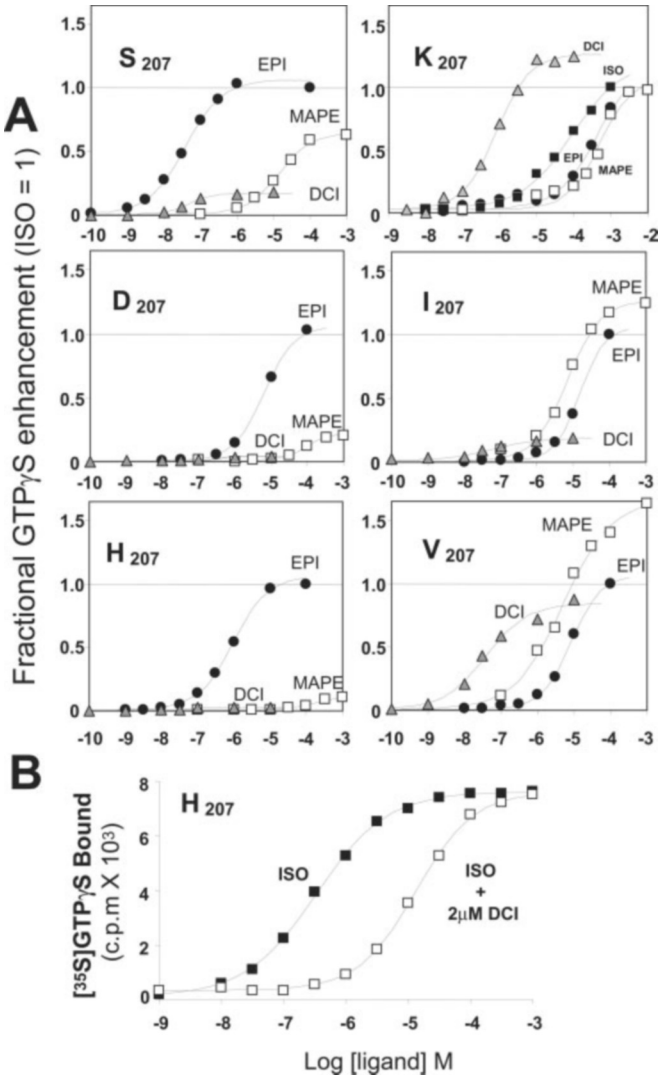


FIG. 9. **Changes of ligand intrinsic activities induced by selected mutations.** *A*, HEK-293 cells were transfected with wild-type (*S207*) and the mutants producing the largest shifts in ligand-induced maximal activation (*i.e.* Asp, His, Lys, Ile, and Val; see Fig. 8). Concentration-response curves for agonist-induced enhancement of GTPγS binding were determined in each membrane. All data (after subtraction of the binding in the absence of ligand) were expressed as fractions of the maximal stimulation induced by ISO (100 μM, except in Lys-207 1 mM). Best fitting *solid lines* were computed by ALLFIT. Data are from a single experiment that was repeated twice with similar results. *B*, membranes from HEK-293 cells transfected with the His-207 mutant. The concentration-response curves for isoproterenol-induced stimulation of GTPγS binding was determined in the absence and presence of DCI (2 mM). The curves have equal slopes and maximal effects, indicating that DCI acts as a pure competitive antagonist in this receptor mutant.

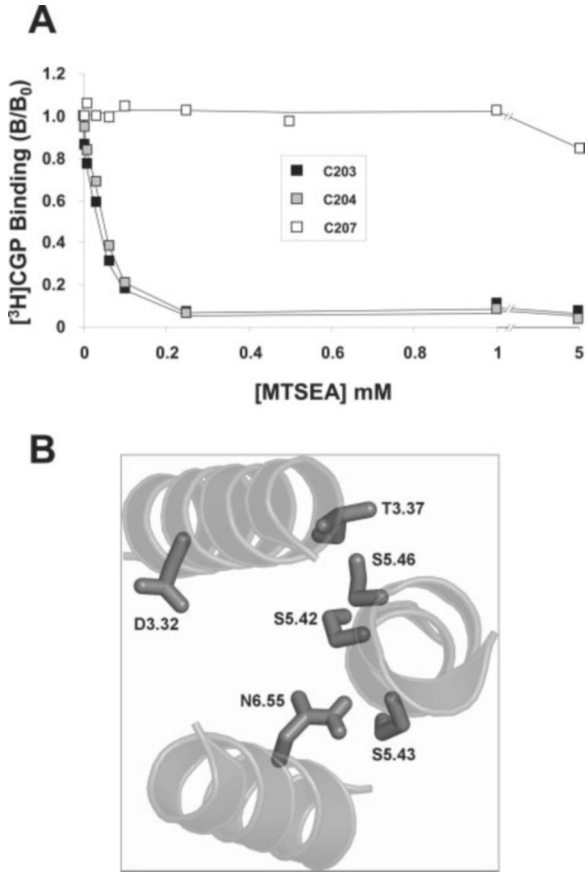


FIG. 10. **Orientation of H5 serines in the wild-type $\beta_2$AR.** *A*, COS7 cells were transfected with either wild-type or the three single Cys mutants S203C, S204C, and S207C of the receptor. Treatment with MTSEA, at the indicated concentrations, and the assessment of the effect on the binding of [³H]CGP-12177 were performed as described in "Experimental Procedures." Data are means of three experiments. *B*, structure of the $\beta_2$AR averaged over the 1000 conformers collected during the last 500 ps of a 1-ns MD trajectory. The extracellular ends of H3, H5, and H6 are represented by *schematics*, whereas the side chains of the binding site aspartate in H3, and of the three serines in H5 and potential interaction partners are represented by *sticks*.

## DISCUSSION

In this study we replaced Ser-207(5.46) in H5 of the human $\beta_2$AR with all other natural amino acids and analyzed the effect of such mutations on binding affinity and efficacy of a number of adrenergic ligands. The results of this work raise three issues that deserve further discussion.

*The Role of Ser-207(5.46) in the $\beta_2$AR*—We may expect that all amino acids replacement of a serine residue that is exposed to the $\beta_2$AR binding cleft and is primarily involved in H–O···H-bonds with catechol hydroxyls, may decrease catecholamine affinity via two overlapping mechanisms. One is loss of the H-bond between the receptor and the ligand, which should predominantly affect the affinity of ligands with a catechol ring. The second, expected instead to affect all ligands (including antagonists and analogues lacking a catechol ring), might be steric hindrance that bulky side chains would exert on the ability of the ligand to enter the binding crevice. Such effect should be more severe, the greater the size of the replaced residue. As shown here, the pattern of effects produced by all-residue substitution of Ser-207(5.46) is far more complex than what we envisioned above. Although catecholamines were indeed affected to a larger extent than other ligands, the observed changes in binding affinities were neither consistent with the mere loss of a ligand-receptor docking interaction, nor with a size-dependent obstruction of ligand entry.

The total span of free energy changes produced by the replacement of serine with the 18 residues ranged from 4.5 (ISO) to 6 (EPI) *RT*-units (equivalent to 11–15 kJ/mol at 25 °C, respectively) for catecholamines, and from 3.4 (MAPE) to 4 (PIN) *RT*-units (*i.e.* 8–10 kJ/mol) for non-catecholic ligands. Because MAPE and PIN cannot form H-bonding with Ser-207(5.46), we suggest that only the difference between the two sets of ranges, *i.e.* 1–2 *RT*-units (2.5–5 kJ/mol), might be attributed to the loss of a putative intermolecular bond between Ser-207(5.46) and the ligand. This is a least estimate, for contributions from hydrophobic effects, side-chain entropy, and, possibly, water intrusion into "cavities" opened by non-isosteric mutations, can heavily affect the ΔΔG values derived from mutagenesis. Despite the uncertainty, such a small value tells that a great part

of energy change that we measure in response to the set of mutations may result from conformational perturbations in the receptor, rather than from the loss of a ligand interaction with a binding subsite.

We also note that the relationship between side-chain identity and change of binding energy for the 4 ligands is not consistent with the presence of a size-dependent clash between the side-chain projecting in the binding cleft and ligand entry. In fact, side-chains bulkier than Ser, either left unchanged (Trp), or actually enhanced (Ile and Tyr) the binding affinity for MAPE, whereas quasi-isosteric changes (Cys and Ala) reduced catecholamine affinity to a larger extent than what the bulkiest residues (*i.e.* Phe, Tyr, and Trp) actually did. Pro, the side chain that caused the largest decrease of affinity for 3 out of 4 ligands, is not bulky, but a well known perturbator of $\alpha$-helix conformation. Finally, there were no significant correlations between the DDG of the 4 ligands and a variety of indicators of side-chain size, including calculated volume, area, bulkiness, Van der Waal size, and partial molar volumes. Such correlations were instead evident for the residue-induced change in receptor expression.

Such observations, taken collectively, raise the question as to whether Ser-207(5.46) projects toward the internal crevice or is rather concealed within the inter-helical interface of H5. MD simulations on empty $\beta_2$AR model indicate that Ser-207(5.46) is the residue most frequently directed toward H3 and involved in H-bonding interactions with T118(3.37). This is consistent with the knowledge that Ser/Thr residues arranged in S*XX*SS or S*XXX*S motifs, particularly if associated to a P in $i+4$ position, are capable to drive strong association between transmembrane helices (12). The prediction that positions 5.46 and 3.37 in $\beta_2$AR are engaged in H-bonding interactions is consistent with rhodopsin structure, where the equivalent positions are, respectively, occupied by H-bonding-linked histidine and glutamate (22, 29). In addition, using SCAM (28), we found that Cys-203(5.42) and Cys-204(5.43) are far more reactive than Cys-207(5.46), which indicates that the side-chain 5.46 is less accessible from the polar cleft than the others in the resting form of the receptor. All the above considerations cast doubts on the otherwise widespread notion that Ser-207(5.46) is available for the formation of a direct H-bond with catecholamines.

One plausible explanation is that Ser-207(5.46) becomes available for ligand docking only during the dynamics of ligand entry. We reported a strong cooperativity between mutation of each of the three H5 serines and changes of the catecholamine structure that affect contacts at other sites of the receptor (7). That suggests the existence of an "induced fit" mechanism in catecholamine binding, so that initial contacts between ligand and receptor synergistically induce the exposure of additional docking points. Thus, the Ser-207(5.46) side chain may turn and interact with the ligand only after initial interactions between the ligand and other subsites of the receptor are established. If so, the residue would not be detectable by the cysteine accessibility method, because the thiol reagent enters the cleft without interacting with the receptor subsites that trigger its exposure. This mechanism agrees with the multistep kinetics of catecholamine-receptor interactions observed in fluorophor-labeled $\beta_2$AR (8). Recent molecular dynamics simulations of the $5HT_{1A}$ receptor in empty and agonist-bound forms suggest a similar mechanism (20). Only after the "primary" interactions with D3.32 and S5.42 are established, is serotonin found to form additional "secondary" interactions with residues in H6 (F6.51) and H5 (T5.43), which occur concurrently with the maximal destabilization of the salt bridges involving the DRY arginine in the cytosolic extension of H3, a hallmark of receptor activation (20). Thus, a stepwise agonist-binding process might be the general feature of all amine GPCRs and play a crucial role in the process of agonist-induced activation.

*Helix-5 Can Trigger Different Modes of Receptor Activation*—Regardless of the orientation of Ser-207(5.46) in wild-type receptor, the substitution of this residue by all natural amino acids has vast effects on the process of receptor activation. Four main receptor phenotypes were generated by mutagenesis as follows: (*a*) complete loss of ligand-induced receptor activation, more effectively caused by Leu, Asn, and Met; (*b*) enhanced activation by catecholamines with reduced responsiveness to non-catecholic agonists, caused by Asp and His; (*c*) enhanced response to non-catecholic ligands, with catecholamines becoming partial agonists, caused by Val, Ile, Ala, and Lys; and (*d*) constitutive receptor activation, caused by Ile and Lys.

Peculiar to the data is the simultaneous occurrence of two opposite trends. Very similar side chains produced large functional differences, whereas unrelated residues caused equivalent functional outputs. Examples of the first case are the pairs Ile and Leu (the first causing constitutive activation, and the second total inactivation), or Asp and Glu (inducing, respectively, enhanced catecholamine responsiveness and inactivation). Examples of the second case are His and Asp (both enhancing receptor activation), or Lys and Ile (both producing constitutive activation). A detailed molecular modeling of the 18 receptor mutants is under way, and hopefully may bring more insight. One challenging question is how small structural variations (*e.g.* the change from Ile to Leu side chain) can make the difference between constitutive activation and full inactivation.

Although not allowing to draw a precise molecular mechanism, our results clearly suggest that there are at least two alternative pathways that link perturbations in position 5.46 to the molecular changes underlying the active form of the receptor. One is represented by the replacement of the two polar residues, His and Asp, which dramatically enhance the activation induced by catecholamines and suppress that mediated by non-catecholic ligands, with no enhancement of constitutive activity. The other is the substitutions with the aliphatic residues, Val, Ile, and Ala, or the charged residue Lys, all of which magnify the activation induced by non-catecholic partial agonists, and half of which also produce ligand-independent activation. This has two interesting implications.

One is that catecholic and non-catecholic agonists may activate the wild-type receptor by different mechanisms, thus, the two groups of mutations may reflect changes that preferentially facilitate either one or the other type of process. Hints on the molecular basis of such differences come from studies on rhodopsin. Solid-phase NMR analysis of the dark- and light-activated rhodopsin forms show that retinal translation toward H5 in the region of His-211(5.46) may be a first move for light-induced conformational changes (30). Enhanced ligand contacts in this area of H5 would break the inter-helical interactions between H3 and H5 and move this helix into an active conformation. It was suggested that such mechanism may be general for all class-A receptors, including $\beta_2$AR. This is in line with the hypothesis that Ser-207(5.46) forms a helix-ligand contact only after the motion generated by initial catecholamine interactions with subsites in H3, H6, and, possibly, S5.42 in H5. This "induced" Ser-207(5.46) contact may boost or modify the consequences of the ligand's interaction with H6, where rigid body movement and outward rotation of the helix are known to be key elements of activation (20, 30–32). The conditional exposure of S5.46 would also be consistent with the induced fit mechanism (7) and the multistep activation kinetics (8) of catecholamines discussed above. In contrast, non-catechol

partial agonists, lacking the Ser-207(5.46) interaction, must be inducing H6 motion without the additional connection with H5, which is likely to result in a different type of motion of this helix relative to the others. A second implication is that constitutive receptor activity and agonist-dependent activation can originate from different structural changes, and therefore do not reflect identical receptor forms.

In fact, among the four mutations that enhanced partial agonist effects, at least two also produced ligand-independent activity. Therefore, the constitutively active receptor form shares more similarities with that bound to a partial agonist than that bound to a full agonist. If so, we may suggest a fundamental difference in the way partial and full agonists activate receptors. Although the partial agonist might simply be a "catalyst" of the intrinsic constitutive activity restrained within the unbound receptor form, the full agonist may act differently, generating a "new" highly dynamic form of the receptor, which substantially differs from the active configurations that the receptor infrequently explores in the unbound state.

*Differences between Partial and Full Agonism*—Ligands that bind to a G protein-coupled receptor (GPCR) display wide variations in their power to trigger receptor activation. This intrinsic ligand/receptor property, known as efficacy (33), ranges from full agonism to inverse agonism. Differences in efficacy are usually attributed to the variable extent to which a ligand can induce an optimal receptor configuration for G protein activation. Although it is likely that each ligand generates on binding a unique receptor conformation, a common subset of perturbations that are relevant to G protein activation are thought to be shared to variable degrees by different ligands, which results in different grades of receptor activation. Thus, efficacy is viewed as a continuous gradient of changes in the active configuration of the receptor, which seamlessly occur within other physical modifications induced by ligand binding, and reaches the top at the full agonism level. Consequently, affinity and efficacy often appear as properties that have independent and distinct structural requirements (34).

Our data prospect two interesting deductions, on this matter. First, the observations that point mutations in a residue of the agonist binding pocket can either switch the full agonist into a partial one, or do the reverse, suggest that full and partial agonists activate the receptor via qualitatively different mechanisms. In fact they easily diverge as even the most subtle modification alters the stereochemistry of ligand-receptor interactions. Similar conclusions were reached from the comparison of the relation between GTP-shift on binding and GTPase activation in a series of $\beta_2$AR agonists (35) and from the analysis of fluorescence lifetime distributions of fluorophor-labeled $\beta_2$AR bound to different agonists (36).

Second, the findings that some mutations can enhance the extent of G protein activation induced by catecholamines indicate that the active configuration triggered by full agonist binding does not constitute the up most level of receptor activation. Larger effects are in fact possible with certain modifications of residue 5.46.

The "hyperactive" mutants His and Asp, although displaying a greater level of activation than wild-type receptor, bind full agonists with reduced affinity. Therefore, at lower agonist concentrations they respond far less than a wild-type receptor. Thus, it appears that the configuration of the active "full agonist form" is not the one having the greatest level of activation but is the one optimized to achieve the best activation with the best binding affinity for the natural ligand. Such an outcome, perhaps resulting from the stepwise dynamics of the full agonist interaction with the receptor, implies a perfect match between ligand structure and receptor structure, which cannot be emulated by mutations that enhance the intrinsic constitutive activity of the receptor.

*Acknowledgment*—We thank T. Lazaridis for letting us probe the IMM1 model.

REFERENCES

1. Strader, C. D., Sigal, I. S., Candelore, M. R., Rands, E., Hill, W. S., and Dixon, R. A. (1988) *J. Biol. Chem.* **263,** 10267–10271
2. Strader, C. D., Candelore, M. R., Hill, W. S., Sigal, I. S., and Dixon, R. A. (1989) *J. Biol. Chem.* **264,** 13572–13578
3. Sato, T., Kobayashi, H., Nagao, T., and Kurose, H. (1999) *Br. J. Pharmacol.* **128,** 272–274
4. Liapakis, G., Ballesteros, J. A., Papachristou, S., Chan, W. C., Chen, X., and Javitch, J. A. (2000) *J. Biol. Chem.* **275,** 37779–37788
5. Ambrosio, C., Molinari, P., Cotecchia, S., and Costa, T. (2000) *Mol. Pharmacol.* **57,** 198–210
6. Del Carmine, R., Ambrosio, C., Sbraccia, M., Cotecchia, S., Ijzerman, A. P., and Costa, T. (2002) *Br. J. Pharmacol.* **135,** 1715–1722
7. Del Carmine, R., Molinari, P., Sbraccia, M., Ambrosio, C., and Costa, T. (2004) *Mol. Pharmacol.* **66,** 356–363
8. Swaminath, G., Xiang, Y., Lee, T. W., Steenhuis, J., Parnot, C., and Kobilka, B. K. (2004) *J. Biol. Chem.* **279,** 686–691
9. Liapakis, G., Chan, W. C., Papadokostaki, M., and Javitch, J. A. (2004) *Mol. Pharmacol.* **65,** 1181–1190
10. Ballesteros, J. A., Deupi, X., Olivella, M., Haaksma, E. E., and Pardo, L. (2000) *Biophys. J.* **79,** 2754–2760
11. Deupi, X., Olivella, M., Govaerts, C., Ballesteros, J. A., Campillo, M., and Pardo, L. (2004) *Biophys. J.* **86**(1 Pt 1), 105–115
12. Dawson, J. P., Weinger, J. S., and Engelman, D. M. (2002) *J. Mol. Biol.* **316,** 799–805
13. Molinari, P., Ambrosio, C., Riitano, D., Sbraccia, M., Gro, M. C., and Costa, T. (2003) *J. Biol. Chem.* **278,** 15778–15788
14. Seifert, R., Wenzel-Seifert, K., and Kobilka, B. K. (1999) *Trends Pharmacol. Sci.* **20,** 383–389
15. Javitch, J. A., Fu, D., Liapakis, G., and Chen, J. (1997) *J. Biol. Chem.* **272,** 18546–18549
16. De Lean, A., Munson, P. J., and Rodbard, D. (1978) *Am. J. Physiol.* **235,** E97–E102
17. Munson, P. J., and Rodbard, D. (1980) *Anal. Biochem.* **107,** 220–239
18. Sali, A., and Blundell, T. L. (1993) *J. Mol. Biol.* **234,** 779–815
19. Okada, T., Sugihara, M., Bondar, A. N., Elstner, M., Entel, P., and Buss, V. (2004) *J. Mol. Biol.* **342,** 571–583
20. Seeber, M., De Benedetti, P. G., and Fanelli, F. (2003) *J. Chem. Inf. Comput. Sci.* **43,** 1520–1531
21. Greasley, P. J., Fanelli, F., Scheer, A., Abuin, L., Nenniger-Tosato, M., De-Benedetti, P. G., and Cotecchia, S. (2001) *J. Biol. Chem.* **276,** 46485–46494
22. Noda, K., Saad, Y., Graham, R. M., and Karnik, S. S. (1994) *J. Biol. Chem.* **269,** 6743–6752
23. Lazaridis, T. (2003) *Proteins* **52,** 176–192
24. Brooks, B. R., Bruccoleri, R. E., Olafson, B. D., States, D. J., Swaminathan, S., and Karplus, M. (1983) *J. Comput. Chem.* **4,** 187–217
25. Ballesteros, J. A., and Weinstein, H. (1995) *Methods Neurosci.* **25,** 366–428
26. Charton, M. (1990) in *Progress in Physical Organic Chemistry* (Taft, R. W., ed) pp. 163–284, John Wiley & Sons, Inc., New York
27. Samama, P., Cotecchia, S., Costa, T., and Lefkowitz, R. J. (1993) *J. Biol. Chem.* **268,** 4625–4636
28. Javitch, J. A., Li, X., Kaback, J., and Karlin, A. (1994) *Proc. Natl. Acad. Sci. U. S. A.* **91,** 10355–10359
29. Teller, D. C., Okada, T., Behnke, C. A., Palczewski, K., and Stenkamp, R. E. (2001) *Biochemistry* **40,** 7761–7772
30. Patel, A. B., Crocker, E., Eilers, M., Hirshfeld, A., Sheves, M., and Smith, S. O. (2004) *Proc. Natl. Acad. Sci. U. S. A.* **101,** 10048–10053
31. Meng, E. C., and Bourne, H. R. (2001) *Trends Pharmacol. Sci.* **22,** 587–593
32. Farrens, D. L., Altenbach, C., Yang, K., Hubbell, W. L., and Khorana, H. G. (1996) *Science* **274,** 768–770
33. Kenakin, T. (2002) *Nat. Rev. Drug Discov.* **1,** 103–110
34. Kenakin, T., and Onaran, O. (2002) *Trends. Pharmacol. Sci.* **23,** 275–280
35. Seifert, R., Wenzel-Seifert, K., Gether, U., and Kobilka, B. K. (2001) *J. Pharmacol. Exp. Ther.* **297,** 1218–1226
36. Ghanouni, P., Gryczynski, Z., Steenhuis, J. J., Lee, T. W., Farrens, D. L., Lakowicz, J. R., and Kobilka, B. K. (2001) *J. Biol. Chem.* **276,** 24433–24436
37. Chotia, C. (1975) *J. Mol. Biol.* **105** 1–14
38. Eisemberg, D., Weiss, R. M., Terwilliger, T. C., and Wilcox, W. (1982) *Faraday Symp. Chem. Soc.* **17,** 109–120
39. Manavalan, P., and Pannuswamy, P. K. (1976) *Nature* **275,** 673–674
40. Grantham, R. (1974) *Science* **185,** 862–864
41. Zamyatin, A. A. (1972) *Prog. Biophys. Mol. Biol.* **24,** 107–123
42. Eriksson, L., Jonsson, J., Sjostrom, M., and Wold, S. (1988) *Quant. Struct.-Act. Relat.* **7,** 144–150